

Overview of Electric Propulsion Activities in Japan

Kimiya Komurasaki¹

The University of Tokyo, Kashiwa, 277-8561, Japan

and

Hitoshi Kuninaka²

Japan Aerospace Exploration Agency, Sagami-hara, 299-8510, Japan.

Cathode-less ion engines are on the Hayabusa asteroid explorer, and Kaufman-type engines are on the Engineering Test Satellite-VIII at present. A 5kW-class Hall thruster and a 200mN-class ion engine are under development. PPTs and laser micro-thrusters are prepared for the propulsion system of microsattellites. This paper reports the recent activities on electric propulsion conducted in Japanese universities, industries, and JAXA.

I. Space Missions

A. Hayabusa Asteroid Explorer (ISAS/JAXA)

The Hayabusa space mission is focused on demonstrating the technology needed for a sample return from an asteroid and was launched in May 2003. The cathode-less electron cyclotron resonance ion engines, which were developed by the Electric Propulsion Laboratory ISAS/JAXA, propelled the Hayabusa asteroid explorer as illustrated in Fig.1. It reached a distance of 0.86 AU from Sun in February 2004 and 1.7 AU from Sun in February 2005. These distances are the farthest that an electric propulsion system has yet attained in the solar system. Depending on the solar distance the ion engines were operated between 250 W and 1.1 kW in electrical power. It is identified that a single thruster generates the swirl torque 2×10^{-6} Nm. It succeeded in rendezvousing with the asteroid Itokawa in September 2005 after a 2-year flight, producing a delta-V of 1,400 m/s, while consuming 22 kg of xenon propellant and operating for 25,800 hours.¹ After a series of scientific observations the Hayabusa landed on and lifted off the asteroid in November 2005 (see Fig.1). Though the spacecraft was seriously damaged and lost the functions of the hydrazine thrusters and two of three reaction wheels after the successful proximity operation, the xenon cold gas jets from the ion engines rescued the Hayabusa. The new attitude stabilization method using a single reaction wheel, the ion beam jets, and the solar pressure was established and enabled the homeward journey aiming the Earth return on 2010. The total accumulated operational time of the ion engines reaches 28,000 hours at the end of May 2007. One of four thrusters, which has been most frequently used, reaches 12,000 hours in space operation. Figure 2 presents the details of the operational time of ion engines and propellant consumption during 4 years. The Hayabusa will come back Earth in 2010 after two revolutions around Sun in the method of the powered flight by the ion engines with 700 m/s delta-V and 10,000-hour operation in addition.²



Fig.1 The powered flight of Hayabusa in deep space (left), and a photo of the Shadow of Hayabusa on surface of asteroid(right).

¹ Associate Professor, Department of Advanced Energy, Kashiwanoha 5-1-5, Kiban 304, Member AIAA.

² Professor, Japan Aerospace Exploration Agency, Yoshinodai 3-1-1, Member AIAA.

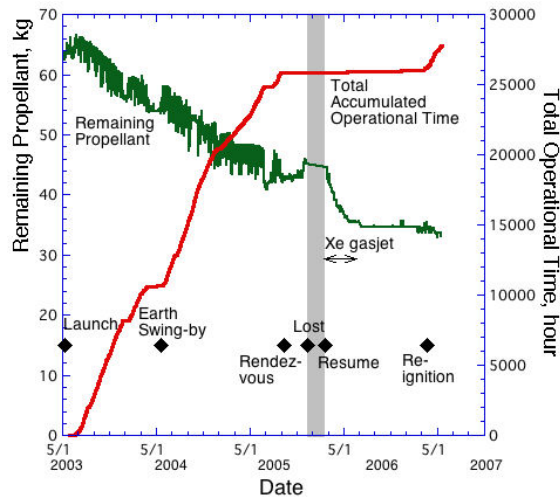


Fig.2 Details on operational time of ion engines and propellant consumption during 4 years.

B. Engineering Test Satellite-VIII (JAXA)

The Engineering Test Satellite-VIII (ETS-VIII) launched in December 2006. It is a three-ton class geostationary satellite utilizing four ion engines for North-South Station Keeping(NSSK). (Fig. 3) Two of them, NA and NB are on the north edge of the anti-earth panel, and the others, SA and SB are on the south edge of the same panel. Either NA or NB thruster is fired around the ascending node (AN), while either SA or SB thruster around the descending node (DN) of the orbit. Each firing time around the AN and the DN is about 1,600 hours a year for NSSK. The major engine specifications are shown in Table 1. Although its thruster design was similar to those on ETS-VI launched in 1994 or COMETS launched in 1998, it was a little modified to extended its lifetime from 8,000 hours to 16,000 hours to meet ten-year operation of ETS-VIII in orbit.

Figure 4 shows the block diagram of the ion engine system. A pressure regulator and flow control modules are used to regulate Xe propellant flow. There are two power processing unit, PPU-A and PPU-B. PPU-A is connected to NA or SA thruster by switching relays. The primary system is the combination of PPU-A, NA thruster and SA thruster. Gimbal mechanism is used to align thrust vector to the satellite's center of mass and to avoid the occurrence of rotation torques.

The ion engine system was checked out in orbit in January 2007 as tabulated in Table 2. Main discharge current and beam voltage were increased step-by-step to nominal level so as to minimize the high voltage breakdown due to trapped gas and out-gassing. After then, normal NSSK operations have been carried out almost every day since March 2007. The operation time

is about six hours around the ascending node and descending node.

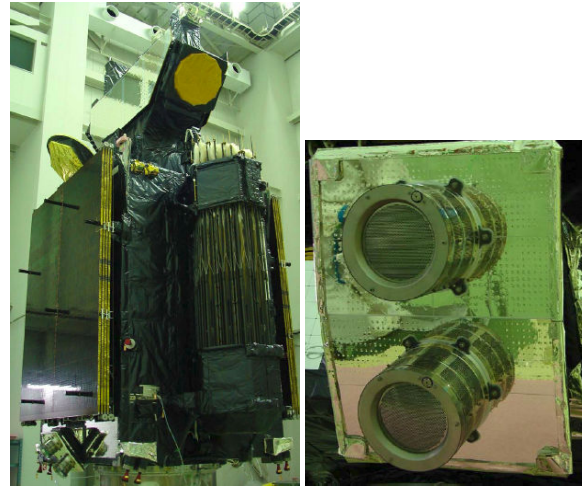


Fig. 3 Ion thrusters on ETS-VIII.

Table 1 Major specifications of ETS-VIII ion engine.

Thruster type	Kaufman-type
Average thrust	>20mN
Average Isp	>2,200sec
Weight	96kg
Operation time	16,000hours
Total impulse	>1.15×10 ⁶ Ns
Number of firing	3,000cycles
Power consumption	<880W
Grid diameter	12cm

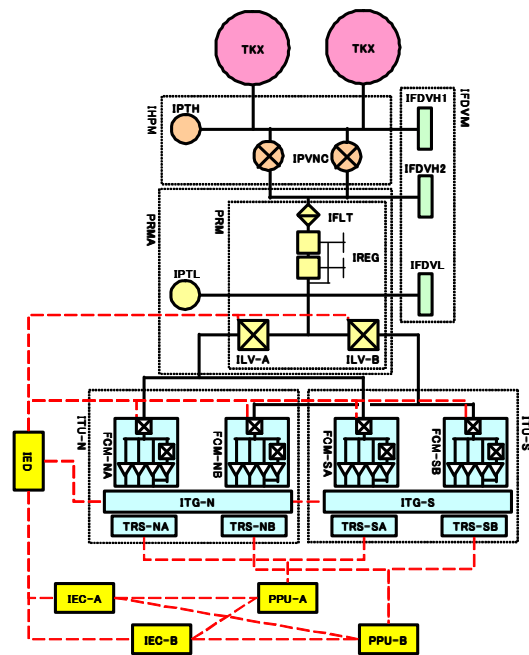


Fig. 3 Brock diagram of ETS-VIII ion engine system.

Table 2 Checked items in-orbit.

- | |
|--|
| 1) Idling Mode (Cathode heater Low Level on) |
| 2) Activation Mode (Cathode heater High Level on) |
| 3) Neutralizer Mode (Neutralizer on) |
| 4) Discharge Mode (Main Discharge on) |
| 5) Grid Cleaning Mode |
| 6) Beam Mode (ion acceleration) : Firing time
NA:11h35m, NB:7h51m, SA : 11h52m, SB: 7h59m |

II. Flight Model Developments

A. MELCO Hall Thruster³

A hall thruster and a power-processing unit (PPU) have been developed since 2003 as a national project under the contract of Institute for Unmanned Space Experiment Free Flyer (USEF) sponsored by Ministry of Economy, Trade and Industry (METI). The target specification is as follows: the thrust level is over 250mN, the specific impulse is over 1,500s under the PPU power consumption of below 5kW, and the lifetime is over 3,000 hours. Mitsubishi Electric Corporation designed, fabricated and evaluated the thruster EM and PPU EM. (Fig. 5)



Fig. 5 200mN class hall thruster EM and PPU EM.

The thruster EM showed the thrust level of 264mN, the specific impulse of 1,720s under the thruster input power of 4.56kW. The thrust ranges from 87mN to 293mN, and the specific impulse does from 1070sec to 1910sec under the input power range from 1.49kW to 5.46kW.

The PPU EM consists of main power conditioners (PCs) such as anode PC, hollow cathode keeper PC, two electromagnetic coil PCs, and primary bus interface. It is designed for 100V regulated satellite bus. It showed over the total efficiency 93% at the output power range from 1.75kW to 4.5kW and at the anode voltage range from 250V to 350V. On the basis of the

results, the thruster EM2 and PPU EM2 are under development.

B. Next-Generation Ion Engine (IAT, JAXA)⁴⁻⁶

The next-generation ion engine shown in Fig. 6 performs very high performance over the wide thrust range from 80 to 200 mN. The most important feature of the thruster is its large-sized ion extraction system, whose diameter is 35 cm. We have improved the ion optics through various performance tests.

Since sufficiently high thruster performance has already been achieved, current efforts are directed to evaluation of reliability and durability of the thruster. A life test of a main hollow cathode was started in March 2006. The high electron-emission capability of over 20 A and the anti-erosion graphite materials are its key features. In this test, the cathode was operated in a dummy discharge chamber whose geometrical and magnetic configuration were almost the same as the actual thruster. (Fig.6). A dummy grid with a limited rectangular open-area was attached on the discharge chamber to regulate the plenum pressure. Figure 7 shows voltage variations and accumulated operation time. Except for some troubles in peripherals, the cathode operation itself has been very stable and favorable. Accumulated cathode-operation time reached 8800 hours in the mid of May 2007 and the operation will be continued until fatal troubles occur.

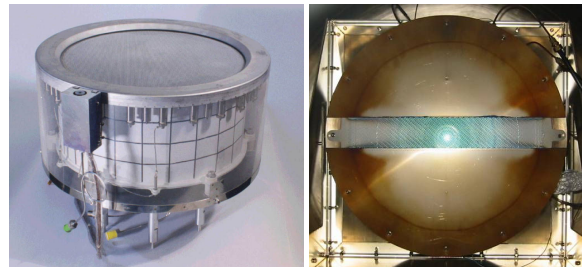


Fig. 6 BBM of the next generation ion engine (left), and hollow cathode discharge in the life test (right).

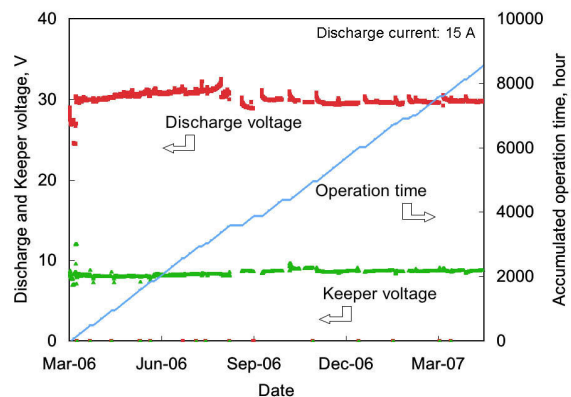


Fig. 7 Voltage variations and accumulated operation time in the life test.

Grid erosion is the most important factor that determines thruster life. In order to estimate the grid life by numerical simulations, beamlet formation should be described precisely. Distribution of ion-impingement current on an accelerator grid was measured using a specially made gridlet shown in Fig. 8. The gridlet was composed of both barrel and downstream electrodes, which were electrically isolated from each other. The results will provide reference data to verify and improve a numerical model.

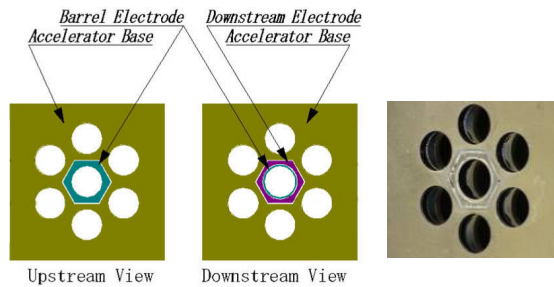


Fig. 8 Accelerator gridlet for the beam extraction test.

C. Pulsed Plasma Thruster for Small Satellites (Tokyo Metropolitan University)^{7,8}

Pulsed Plasma Thrusters have been developed for the application to 50kg-class small satellites. Following the R&D of a parallel electrode (rectangular) PPT, TMU has begun to study a co-axial PPT. Owing to its electromagnetic acceleration, a parallel electrode PPT shows the high specific impulse and very small impulse-bit, which would be advantageous for the attitude control and precise orbit control of satellites. On the other hand, a co-axial PPT, in which electrothermal acceleration is dominant, shows large impulse-bit (nearly 1mN) and high thrust efficiency. It is favorable for the station-keeping and de-orbit. Wide performance range (20 μ N-s impulse bit, 2,000 s Isp to 1mN-s impulse bit, 14 % thrust efficiency) has been achieved as shown in Figs.9 and 10.

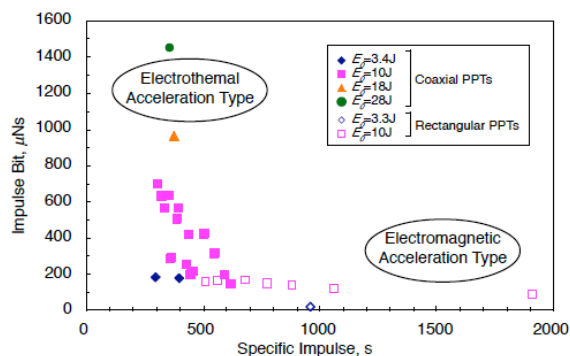


Fig. 9 Performance summary of rectangular (electromagnetic) / coaxial (electrothermal) type of PPT.

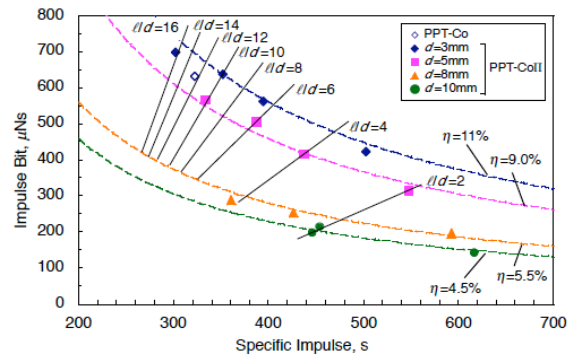


Fig. 10 Effects of aspect ratio of a coaxial PPT discharge chamber.

D. Microwave Discharge Ion Thrusters (ISAS/JAXA)

In order to advance the technology of cathode-less microwave discharge ion engines known as the “ μ ” family, two programs are being carried out: μ 20 and μ 10Hisp. The former is a 20-cm diameter engine, and the latter is a higher specific impulse version of the 10-cm diameter μ 10. Table 3 summarizes the achieved and the target performance of the models.

Table 3 Performance of “ μ ” series ion thrusters.

Items	μ 10 achieved	μ 20 target	μ 10Hisp target
Ion Prod. Cost, W/A	230	200	230
Beam Current, mA	140	500	140
Microwave Power, W	32	100	32
Beam Voltage, V	1,500	1,200	15,000
Specific Imp., sec	3,000	2,800	10,000
Thrust, mN	8.5	27	27
System Power, W	350	900	2,500
Thrust/Power, mN/kW	22	30	11

The performance of μ 20 was improved by the combination of a thin screen grid and an optimized gas injector & magnet layout. Though specific impulse and propellant utilization efficiency still remained conservative, the thrust-to-power ratio was successfully increased from the μ 10’s level of 22 mN/kW to 30 mN/kW.⁹ We measured two-dimensional distributions of E-field and electron temperature inside the discharge chamber, and the ion beam profiles downstream the optics (Figs 11). All the parameters in the worst performance case showed very uniform distributions. On the other hand, in the best case, obvious peaks were observed for all the parameters.

Aperture diameter of an accelerator grid was designed for improvement of propellant utilization efficiency. Evaluation of this new optics and the 1000-hour wear test of μ 20 system are planned in this summer.

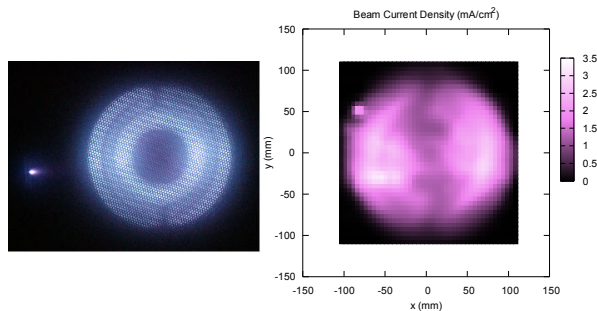


Fig. 11 Front view of the operating $\mu 20$ and its beam current density profile.

The potential application of the $\mu 10$ Isp is a solar-electric sail mission to Jupiter, which requires solar electric propulsion system with Isp of 10,000sec achievable using beam voltage of 15kV. Operation of the $\mu 10$ Isp was demonstrated in the laboratory (Fig.12) using high voltage insulation techniques such as a DC block, gas isolator and supporting elements. Although Isp of over 9,000sec was achieved,¹⁰ it has not reached 10,000sec yet because of relatively large drain current of 20mA to an accel grid. It is thought that the non-uniform ion current distribution causes direct impingement of ions to the accel grid due to cross over limit. By suppressing the impingement, 10,500sec Isp, 29mN thrust, 11.2mN/kW thrust power ratio and 58% total efficiency would be expectable. A power processing unit for the $\mu 10$ Isp is under development in corporation with NTSspace.

DC blocks, which transmit microwaves to ion sources and neutralizers damming up DC voltages, are very important components. A low-insertion-loss DC block with a withstanding voltage of 3 kV is under development for $\mu 10$ and $\mu 20$ to improve electrical efficiencies and to increase mechanical strength with a support of new energy and industrial technology development organization (NEDO) under the industrial technology research grant program. Several laboratory models are now under a thermal cycling test and will be integrated to the $\mu 20$ system for a 1000-hour wear test.

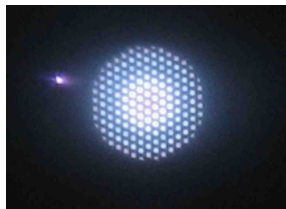


Fig. 12 Front view of the operating $\mu 10$ Isp.

E. Project of Osaka Institute of Technology Electric-Rocket-Engine onboard Small Space Ship

The Project of OIT Electric-Rocket-Engine onboard Small Space Ship (POERESSS) was started. A 10-kg

small satellite with electrothermal PPTs, named JOSHO, will be launched in 2010. An orbit raising and attitude control of JOSHO in LEO will be carried out by the PPTs. Their endurance test is under way.

An electrothermal PPT with a side-fed propellant feeding mechanism was tested. Initial thrust-to-power ratio of 43-48 $\mu\text{Ns/J}$ ($\mu\text{N/W}$), Isp of 470-500 sec and thrust efficiency of 11-12 % with stored energy of 4.5-14.6 J per shot, and a total impulse of 3.6 Ns were obtained in a repetitive 10000-shot operation with a stored energy of 8.8 J per shot.

F. Diode Laser Microthruster^{11,12} (The University of Tokyo)

Two types of diode laser microthrusters with different propellants have been developed for 10 cm class microsattellites. One provides total impulse of 30 Ns within the propellant volume of $5 \times 5 \times 6 \text{ cm}^3$ with a single shot impulse of 650 mNs. This thruster will enable a microspacecraft to orbit around mother spacecraft quickly. The other is a thruster of $3 \times 3 \times 2 \text{ cm}^3$, including a diode laser, optics, and micro-motor designed for reaction-wheel un-loading of a 1 kg cube-sat developed by Tokyo Metropolitan College of Aeronautical Engineering, Japan.¹³ Its launch is scheduled in summer 2008 as a piggyback satellite of H-IIA rocket. (Fig. 13)

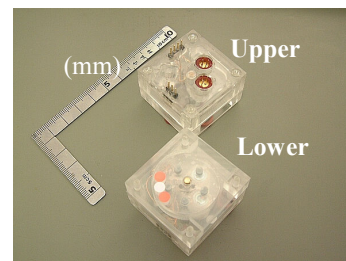


Fig. 13 EM of the laser ignition microthruster

III. Basic Researches

A. Osaka Institute of Technology

1. Hall Thrusters

The laboratory-model thruster THT-III was operated with three channel wall materials of BN, BNSiN, and BNAIN. The axial distributions of wall and plasma potentials, radial and axial electron temperatures, and electron number density near the channel walls were measured. As a result, ionization region and ion wall loss in the channel were found to be affected by the wall material, although ion acceleration region was not. Consequently, the difference in discharge current was considered to be caused by the difference in axial current density near the inner channel wall, depending on the secondary electron emission coefficient of the wall materials.

The cylindrical Hall thruster (CHT) is an attractive approach to achieve long lifetime especially in low power applications. Because of the larger volume-to-surface ratio than conventional coaxial Hall thrusters, CHTs are characterized by a reduced heating rate of thruster components and by a lower erosion rate of the channel. The 5.6-cm-diameter thruster TCHT-3B was operated, as shown in Fig.14(a), in the power range of 30-150 W to examine the effects of magnetic field configuration. By adjusting the axial position where a large magnetic field is applied in the channel, TCHT-3B achieved a high efficiency of 18-39%.

The effects of magnetic field topography and discharge channel structure on performance were experimentally examined using a 1-kW-class anode-layer Hall thruster TALT-2 as shown in Fig.14(b). The performance enhancement using a divergent-type hollow anode was confirmed under the optimum channel length and various magnetic field topographies created by magnetic shields and a radial trim coil. As a result, thrust efficiency was enhanced to 57 % with the divergent-type hollow anode at a discharge voltage of 400 V and a xenon mass flow rate of 3.0 mg/s.

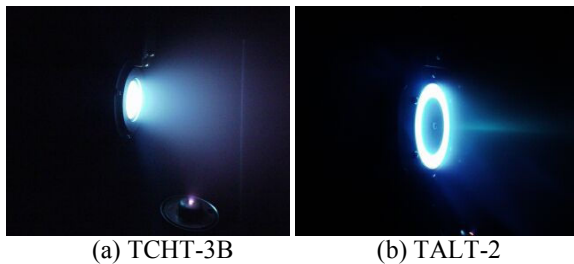


Fig. 14 Photographs of Hall thruster operations.

2. Electrothermal PPT with multiple cavities

An electrothermal PPT with multiple cavities (discharge rooms) shown in Fig.15 was proposed. It has an igniter and holes for inducing discharges in all cavities. This mechanism was used as a substitute for the propellant feeding mechanism to use a large amount of propellant. A PPT with two cavities showed an initial impulse bit per stored energy of 75 $\mu\text{Ns}/\text{J}$ with a stored energy of 14.6 J and a lower decreasing rate of impulse bit in a repetitive operation than a conventional electrothermal PPT. Furthermore, a PPT with three cavities was successfully operated as shown in Fig.15. This inducing mechanism is applicable to a PPT with larger number of cavities for a higher total impulse.

Unsteady phenomena, such as discharge in the circuit, heat transfer to the PTFE, heat conduction inside the PTFE, ablation from the PTFE surface and plasma flow were simulated numerically. The result showed the existence of considerable amount of ablation delaying to the discharge. However, it was also shown that this phenomenon should not be regarded as

the late time ablation (LTA) for electrothermal PPTs because neutral gas ablated delaying to the discharge generates most of total pressure and impulse bit.

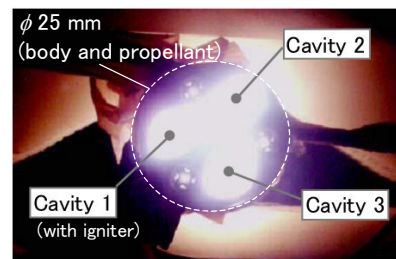
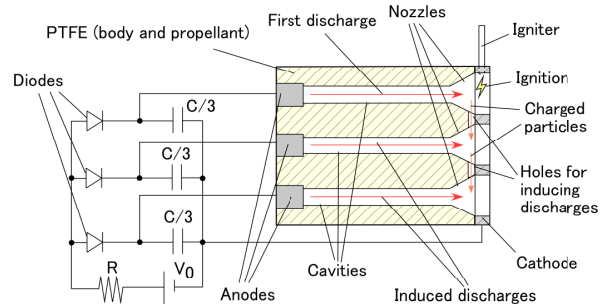


Fig. 15 Conceptual diagram of a multi-cavity electrothermal PPT (top) and the discharge in PPT with three cavities (bottom).

B. Kyushu University

1. Miniature Microwave Discharge Ion Thruster

Miniature microwave discharge ion engines (Fig. 16) are candidates for use as miniature propulsion systems. However, their thrust performance has been far inferior to conventional ion thrusters. For understanding the mechanism of plasma production and loss, internal plasma structure of this was measured and numerically analyzed. These results showed that there is an optimum magnitude of magnetic field due to the tradeoff between a magnetic confinement and a microwave-plasma coupling.

Overall, the thruster performance, propellant utilization efficiency, ion beam production cost, estimated thrust and thrust efficiency were 91%, 611 W/A, 0.79 mN, and 0.58, respectively, at $\dot{m} = 0.020$ mg/s, and $P_i = 8$ W. (Fig.17)

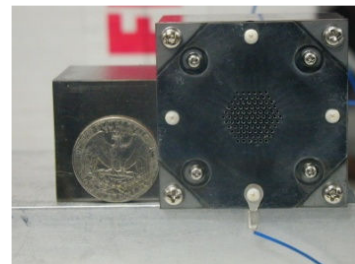


Fig. 16 Miniature microwave discharge ion engine.

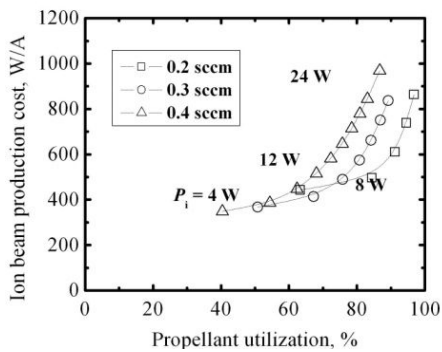


Fig. 17 Thruster performance.

2. 10 cm class Microwave Discharge Ion Thruster

For deep space missions, thrust performance of an argon-propellant microwave discharge ion thruster with a multi-mono-pole antenna system was investigated by changing the magnetic field configuration. The results suggest that there would be optimum magnetic configurations dependent on the propellants.

3. Magnetic Plasma Sail

A magnetic plasma sail is a propulsion system, which travels interplanetary space by capturing the energy of the solar wind using a dipole magnetic field generated by plasma inflation. The plasma inflation and the interaction between the solar wind and inflated magnetic field were calculated by a 3D hybrid simulation code. The result shows that the magnetic field was successfully inflated, but the thrust of this system was estimated as small as 8.6 mN.

4. Hall thruster

Plasma parameters, such as plasma potential, electron temperature and electron number density in an anode layer type Hall thruster were measured by means of an electrostatic probe. The anode layer in which plasma potential is sharply falling was observed under low magnetic field condition, and its axial position moved toward anode with an increase in magnetic flux density. This would lead the movement of an ionization zone toward the anode with magnetic flux density.

C. Tokyo University of Agriculture and Technology

An electrodeless MPD thruster using a compact helicon source with electromagnetic plasma acceleration has been studied for applications to future electric propulsions.¹⁴ They already confirmed the helicon plasma of 10^{-13} cm^{-3} inside a 2.5 cm i.d. glass tube (Fig. 18) and examined the principle of electrodeless electromagnetic acceleration by RF antennae.

For future evolutionary propulsions, TUAT also has started a study of propellant-less propulsion using photon pressure as the motive force.¹⁵ A precision thrust stand discriminating 0.1 μN is being developed

so that a 300 W tungsten filament (as a quasi-black body radiation) with a parabolic mirror demonstrates 1 μN assuming 100 % conversion efficiency directly from electrical to thrust power. (Fig. 19)

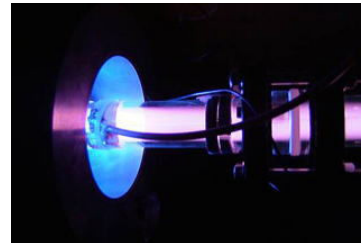


Fig. 18 Compact helicon plasma in blue-mode inside an i.d. of 2.5 cm glass tube.



Fig. 19 A photon pressure thruster using tungsten filament as a primitive experiment.

D. Kyoto University

We have developed a micro plasma thruster of electrothermal type using azimuthally symmetric microwave-excited plasmas,¹⁶⁻¹⁹ which consists of a microplasma source and a micronozzle as shown in Fig. 20. The microwave power would be limited to < 10 W, because of the electric power usable on microspacecraft.

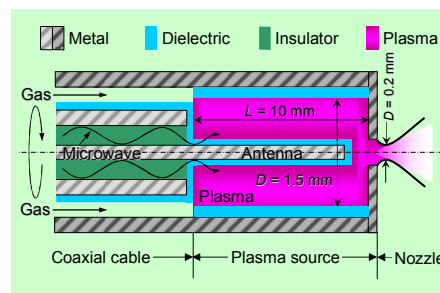


Fig. 20 Micro plasma thruster using microwave-excited surface wave discharges.

We developed a numerical model consisted of an electromagnetic model for microwave propagation in interaction with plasmas and a fluid model for plasma flows with two (electron and heavy particle) temperatures.^{16,19} The former was applied to the plasma source region, to analyze the microwave power absorbed in the plasma; and the latter was applied to both the source and nozzle regions, to analyze the plasma and nozzle flow characteristics in severe

plasma-wall interactions. The working gas of interest was Ar, N₂, and H₂. The micronozzle flow was found to be heavily affected by viscous dissipation in thick boundary layers on the nozzle wall.

The microplasma source was made of a dielectric tube 10 mm long and 1.5 mm in diameter, producing plasmas in the pressure range from 5 to 50 kPa. Optical emission spectroscopy and Langmuir probe measurement showed that the emission intensity, electron density, and rotational temperature of mixed N₂ increased with increasing microwave power ($P_{in}=1-10$ W), frequency ($f=2, 4$ GHz), and dielectric constant ($\epsilon_d \approx 3.8, 6, 12-25$) of the tube.^{17,18} The rotational temperature was found to increase toward the micronozzle to achieve high thrust performance. At $P_{in}=2-10$ W with an Ar gas flow rate of 50 sccm, the electron density and rotational temperature obtained were $n_e \approx 10^{12}-10^{14}$ cm⁻³ and $T_{rot} \approx 700-1800$ K, respectively. These were consistent with the results of numerical analysis.

The micronozzle was fabricated in a 1-mm-thick quartz plate, where the nozzle had an inlet, throat, and exit diameter of 0.6, 0.2, and 0.8 mm, respectively, as shown in Fig. 21(a). Plasma discharges gave an elongated plume of supersonic plasma jet, as shown in Fig. 21(b), downstream of the nozzle exit into vacuum.¹⁹

We also developed a thrust measurement method for micro thrusters of $F_t \leq 1$ mN,¹⁹ consisting of a pendulum-type stand for cold-gas operation and a target-type stand for both cold-gas and plasma-discharge operations. In the former, the thruster itself was hung; in the latter, a small concave target block was hung downstream of the nozzle exit with the thruster fixed tightly. The displacement in operation was measured using a laser displacement gauge. The measurements showed that the thrust and Isp were 1.2 mN and 85 sec, respectively, at $f=4$ -GHz, $P_{in}=9$ W and an Ar flow rate of 50 sccm (1.5 mg/s), being consistent with the numerical analysis. It is concluded that the present micro plasma thruster is applicable for primary and attitude control of micro spacecraft of < 10 kg.

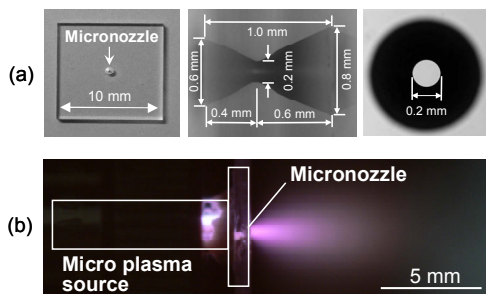


Fig. 21 (a) Microscope image of the micronozzle fabricated, and (b) supersonic Ar plasma jet plume through the nozzle into vacuum ($f=4$ GHz, $P_{in}=5$ W).

E. IAT/JAXA

As a countermeasure against space debris inflation, the research and development of space debris removal systems using electrodynamic tether (EDT) propulsion are being conducted.²⁰ EDT can be a totally propellant-free propulsion system if a bare tether is used as an electron collector and a field emission cathode as an electron emitter. We have been developing some components of the EDT system such as bare tethers, reel mechanisms, field emission cathodes using carbon nanotubes, and others aiming at demonstrating on-orbit operation. Figure 22 shows an image of a debris removal system in near future.

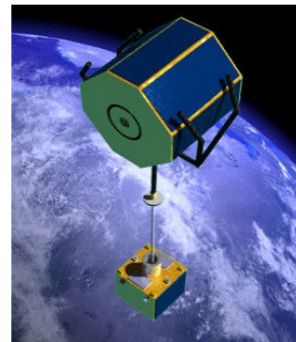


Fig. 22 Image of a debris removal system with electrodynamic tether propulsion. (IAT)

F. Shizuoka University

1. Studies on Electrodynamic Tethers

Shizuoka University is supporting the IAT/JAXA electrodynamic tether deorbit system with analytical and experimental studies.²¹⁻²³

The hybrid tether system in which the electrodynamic tether is used as the orbit restoration system of rotational momentum tether orbit transfer system, is also studied. The results of the mission analysis at present show that the EDT-momentum tether hybrid system can reduce the total system mass by almost 30 % compared with an ion thruster-momentum tether combination for the same missions.²⁴ We are also studying about the new interplanetary transportation system using the electrodynamic tether with a magnetic coil (Fig.23, we call this system “Mag-Tether”) and showed that this system was more effective for the travel beyond the Jupiter than a mag-sail in the initial study.²⁵

2. Interplanetary propulsion system using stardust as propellant

For the travel to outer planets like Jupiter and Saturn, the total mass of the transportation system can be extraordinarily reduced if we can use the interplanetary materials as propellant. We pay attention to the stardust in space as an interplanetary material. The stardust

abundantly exists in the asteroid belt and is easier to be taken than gases in space. To use the stardust as propellant, it is necessary to accelerate effectively solid micro-particles.

We apply the contact charging and the electrostatic acceleration to charge and accelerate solid micro-particles. The experimental study of stardust accelerator (Fig.24) is now undergoing to improve its charging and accelerating performance of the solid micro-particles, and to find the effective way to supply the solid micro-particles.²⁶

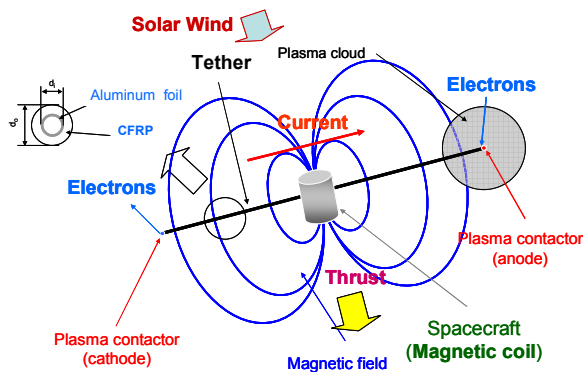


Fig. 23 Conceptual figure of the new interplanetary transportation system using electrodynamic tether with a magnetic coil (Mag-Tether).

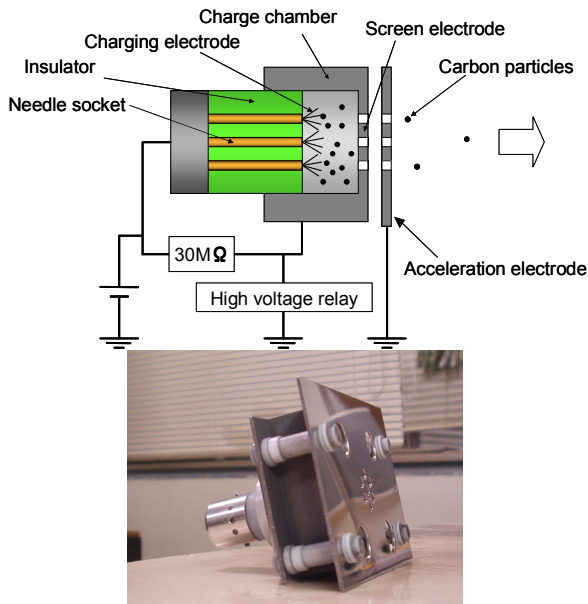


Fig. 24 Conceptual figure and photograph of stardust accelerator.

G. Tokyo Metropolitan University

1. Green Propellant for RCS with Discharge Plasma

Evaluation on hydrogen peroxide and another propellant reaction process with discharge plasma

without catalyst is being carrying on.^{27,28} The objective of this study is to estimate the effects of discharge plasma to the chemical reaction process for the catalyst-less green propellant RCS thruster.

2. Plasma Contactor for Electrodynamic Tether

Evaluations of an electrodynamic tether system using a hollow cathode, another electron emission devices, and bare tether, have been carrying on. Understanding the contacting process with simulated space plasma, it enables various applications of electrodynamic tether system such as orbit raising, de-orbit, station keeping and power generator.

3. Ion Thruster and Hollow Cathode

Fundamental studies on hollow cathode discharge phenomena and electron bombardment ion thruster performance improvement are also keeping on.²⁹ RF ion thruster with RF neutralizer is also evaluated.

H. National Defense Academy

A visualized ion thruster (VIT) was designed and fabricated for evaluation and validation the numerical analysis models, and for the fundamental/educational understanding of an ion thruster. The shape of VIT is two-dimensional rectangular parallelepiped, and the plasma is produced by direct current discharge. The electron produced within an electron source is emitted to the discharge chamber through the keeper bridge plasma. Xenon propellant is ionized by electron bombardment and extracted by a grid system. Figure 25 shows the discharge and three ion beams which were directly observed through the VIT glass plate. It was confirmed that the plasma sheath formed near the grid slit was convex against the grid when the applied screen grid potential was low, and was concave when the potential was high. In addition, it was also confirmed that the electrical connection to the anode/anodes changed the discharge path and influenced the thruster performance.

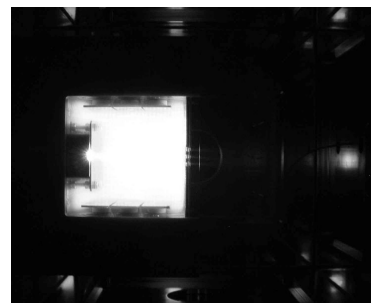


Fig. 25 Discharge and ion extraction of VIT.

I. Nagoya University³⁰

Experimental studies of laser propulsion are conducted. Using the Velocity Interferometer for Any

Reflector (VISAR), the time variations of laser-ablative pressure are measured with a time resolution of 4 ns. The integrated laser-ablative impulse over repetitive laser pulses is measured using a torsion-type impulse balance of a natural frequency of 27 sec. The impulse is almost linear with the laser energy, but has secondary effects caused by ablator morphology. Based on these fundamental results, the vertical launch in a laser-driven, in-vacuum-tube accelerator is successfully demonstrated (see Fig. 26). A TEA (Transversely-Excited Atmospheric) CO₂ laser, 10 J/pulse, 50 Hz at maximum, is used. The ablator is made of polyacetal. The inner diameter of the acrylic launch tube is 25 mm, projectile weighs 6 grams.

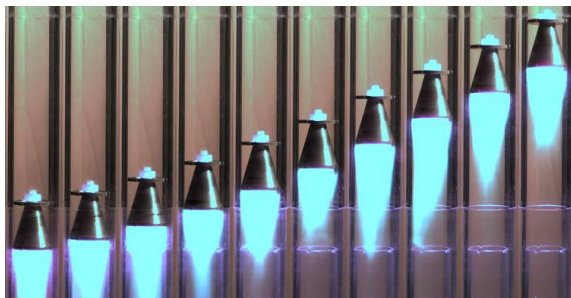


Fig. 26 Vertical launch in laser-driven, in-vacuum-tube accelerator.

J. Tokai University³¹⁻³³

We have been conducting microfabrication of micro-arcjets or -plasmajets with ultra-violet lasers, and development rectangular DC micro-arcjets of various sizes operated under 5 W. The micro-arcjet nozzle was machined in a 1.2 mm thick quartz plate. For an anode, a thin Au film (~ 100 nm thick) was coated in vacuum on a divergent part of the nozzle. As for a cathode, an Au film was also coated on inner wall surface. In operational tests, a stable discharge was observed for mass flow of 0.4 mg/sec, input power of 4 W. In addition, microfabrication of the micro array-nozzle (Fig.27) with UV lasers was conducted.

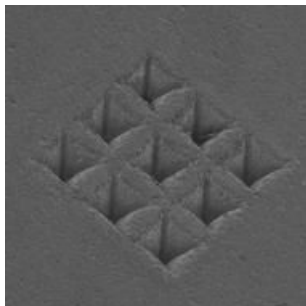


Fig. 27 SEM image of a 3 x 3 micro-arcjet array, in which exit height of each nozzle element is 500 μ m and separations between nozzle edges are 100 μ m.

Moreover, its preliminary thrust characteristics were compared with the single-nozzle as shown in Fig.28. Significant increases of the thrust and Isp with mass flow can be seen in the array-nozzle case.

To elucidate influence of the interaction of exhaust multi-jets on internal flow of the micro array-nozzle, numerical simulation was conducted using a DSMC code. As seen in Fig.29, pressure at the nozzle exit increases through the interaction of exhaust-jet boundaries. This effect must increase static pressure of boundary layers in internal nozzle flows. The boundary layer thickness can be reduced by increasing pressure. Mach numbers drop between the jet-boundaries, and then the exhaust-jets are not expanded at the nozzle exit, or rather confined. These effects will reduce losses derived from viscous losses of internal nozzle flow and under-expanding flow of exhaust jet.

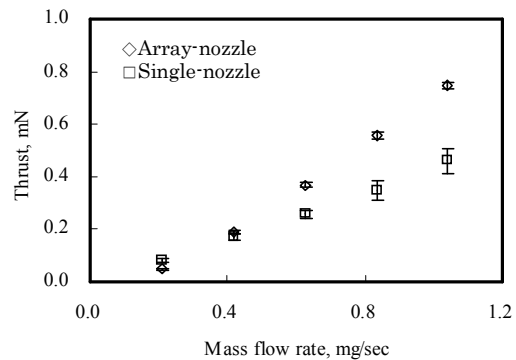


Fig. 28 Comparison of thrusts with single-nozzle and array-nozzle for various mass flow rate.

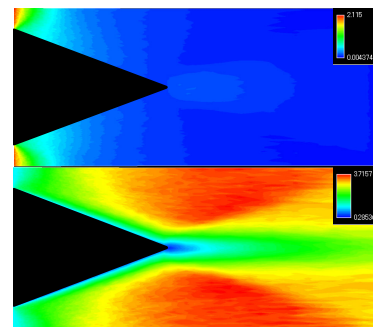


Fig. 29 DSMC computation of internal nozzle flow and exhaust multi-jets. Pressure (top) and Mach number (bottom) distributions.

K. The University of Tokyo

1. Hall Thruster

Sheath structures in an anode-layer thruster was computed using the fully kinetic 2D3V Particle-in-Cell and the DSMC methods.³⁴ The ion production current in an anode hollow is found to decrease with magnetic flux density: At the low magnetic flux density, ion production current in the anode hollow is high and an

ion sheath was created on the anode surface, contributing to the stable discharge.

A two-dimensional dual-pendulum thrust stand (Fig. 30) had been developed to measure a thrust vector of a thruster with steering mechanism.³⁵ A thermal drift effect is canceled out between inner and outer pendulums. Its measurement errors were less than 0.25 mN (1.4%) in the main thrust direction and 0.09 mN (1.4%) in its transversal direction. The steering angle of thrust vector of ± 2.3 degrees was successfully measured with the error of ± 0.2 degree.

Xe density profiles in a plume were measured using laser absorption spectroscopy for the development of a plume shield of a thruster.³⁶ The maximum total number density was $3.9 \times 10^{19} \text{ m}^{-3}$ at the channel exit. Then, the number density decreased by one order at 200 mm away from the exit.

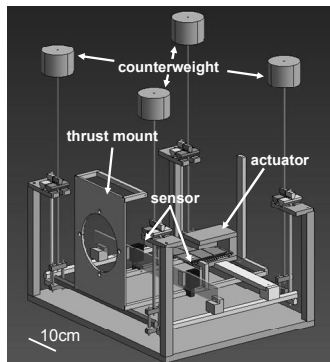


Fig.30 Two-dimensional dual-pendulum thrust stand.

2. Pulsed Plasma Thruster

Liquid propellant is fed using a pulsed liquid injector.³⁷ A spark plug initiator is synchronized with the liquid injection. The single shot impulse was measured using a thrust stand with the resolution of 1.0 μN .³⁸ As a result, Isp of 3,000 sec was accomplished by throttling the single-shot liquid propellant down to 3 μg .

In an ablative PPT, the interaction of the solid wall ablation (propellant feeding) and its ionization and acceleration makes the phenomena more complicated. To fully understand this flow behavior, the acceleration processes were observed by high speed photography (Fig. 31). Monochromatic images were taken at two wavelengths selected for ion and neutral emissions. As a result, it was shown that high density, ablated neutral gas stayed near the propellant surface, and only a fraction of the neutrals was converted into plasma and electromagnetically accelerated, leaving the residual neutrals behind.³⁹

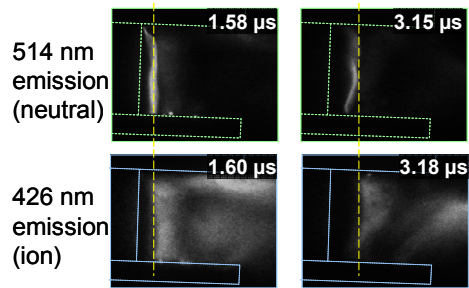


Fig. 31 High speed photography of the ablative PPT (ion and neutral emissions).

L. Tohoku University

A high power magneto-plasma-dynamic thruster (MPDT) operated with a magnetic nozzle has been investigated in detail. Experiments are performed in the HITOP device, which consists of a large cylindrical vacuum chamber (diameter 0.8m, length 3.3m) and 17 magnetic coils. An MPDT shown in Fig.32 is operated quasi-steadily (1ms) with He gas as a propellant. Axial magnetic field is applied to the MPDT and exhaust velocity is measured by a spectrometer in order to clarify the optimum field structure for the applied-field MPDT.

Experiments of both ion cyclotron resonance heating (ICRH) and acceleration in a magnetic nozzle are also performed. This research is related to the VASIMR-type thruster, in which thrust and specific impulse can be changed with constant electric power. When ICRF (ion-cyclotron-range of frequency) waves are excited by a helically-wound antenna, ion temperature T_i drastically increases during the RF pulse. Perpendicular component to the magnetic field of ion energy decreases, whereas parallel component increases along the diverging magnetic field. This indicates that the increased thermal energy is converted to flow energy in a diverging magnetic nozzle. The ion acceleration along the field line is clearly observed in both He and H_2 gases. The exhaust energy can be controlled by input RF power only as shown in Fig.33.



Fig.32 An MPDT with an extended support. This structure is for the optical measurement at the MPD muzzle.

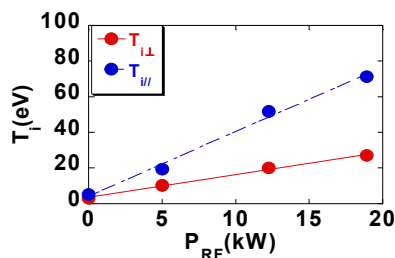


Fig.33 Ion temperature as a function of input RF power. Parallel and perpendicular components to the magnetic field are measured at the end of diverging magnetic nozzle. He plasma. $n_e=10^{17}m^{-3}$.

Acknowledgements

The authors gratefully acknowledge all the Japanese colleagues in universities, industries and JAXA who contributed.

References

¹Kuninaka, H., Nishiyama, K., Funaki, I., Yamada, T., Shimizu, Y., and Kawaguchi, J., "Powered Flight of Electron Cyclotron Resonance Ion Engines on Hayabusa Explorer", *Journal of Propulsion and Power*, Vol.23, No.2, 2007, pp.544-551.

²Kuninaka, H., Nishiyama, K., Shimizu, Y., Hosoda, S., Koizumi H., and Kawaguchi, J., "Status of Microwave Discharge Ion Engines on Hayabusa Spacecraft", AIAA-2007-5196, 43rd Joint Propulsion Conference & Exhibit, Cincinnati, July 2007.

³Ozaki, T., et al., "Electric Propulsion Development Activity at MELCO", 42nd Joint Propulsion Conference and Exhibit, AIAA-2006-4321, Sacramento, CA, 2006.

⁴Ohkawa, Y., Hayakawa, Y., Yoshida, H., Miyazaki, K., Kitamura, S., and Kajiwara, K., "Overview and Research Status of the JAXA 150-mN Ion Engine," 25th International Symposium on Space Technology and Science, ISTS Paper 2006-b22, Kanazawa, Japan, June 2006.

⁵Hayakawa, Y., Yoshida, H., Ohkawa, Y., Miyazaki, K., and Kitamura, S. "Carbon Orificed Hollow Cathodes for Xenon Ion Thrusters," 43rd Joint Propulsion Conference and Exhibit, AIAA Paper 2007-5173, Cincinnati, Ohio, July 2007.

⁶Hayakawa, Y., "Measurements of Current Distribution on a Two-Grid-Ion-Extraction-System Gridlet," 42nd Joint Propulsion Conference and Exhibit, AIAA Paper 2006-5003, Sacramento, California, July 2006.

⁷Uezu J., Iio J., Kamishima Y., Takegahara H., et al., "Study on Pulsed Plasma Thruster Configuration to Expand Impulse Bit Range," 29th International Electric Propulsion Conference (IEPC), Princeton, USA, IEPC-2005-234, October 31-November 4, 2005.

⁸Iio, J., Takegahara, H., et al., "Evaluation on Impulse Bit Characteristics of Pulse Plasma Thruster by Single Impulse Measurement," 29th IEPC, Princeton, USA, IEPC-2005-236, October 31-November 4, 2005.

⁹K. Nishiyama, T. Nakai and H. Kuninaka, "Performance Improvement of the Microwave Discharge Ion Thruster $\mu 20$,"

AIAA-2006-5176, 42nd Joint Propulsion Conference & Exhibit, Sacramento, California, July 2006.

¹⁰H. Hayashi and H. Kuninaka, "Experimental Demonstration of Microwave Discharge Ion Engine with 10,000sec Isp," ISTS-2006-b-33, 25th International Symposium on Space Technology and Science, Kanazawa, Japan, June 2006.

¹¹Koizumi, K., Inoue, T., Arakawa, Y., and Nakano, M., "Dual Propulsive Mode Microthruster Using a Diode Laser," *Journal of Propulsion and Power*, Vol.21 (2005) No.6, pp.1133-1136.

¹²Koizumi, K., Inoue, T., Komurasaki, K., and Arakawa, Y., "Fundamental Characteristics of Laser Ablation Microthruster," *Transactions of the Japan Society for Aeronautical and Space Sciences*, Vol.50, No.167, pp.70-76, 2007.

¹³Nakano, M., Koizumi, H., Inoue, K., Watanabe, M., and Arakawa, Y., "A laser ignition microthruster for microspacecraft propulsion," 25th International Symposium on Space Technology and Science, Kanazawa, Japan, 2006. ISTS-2006-b-05.

¹⁴K. Toki, S. Shinohara, T. Tanikawa, K. Shamrai, T. Hada, I. Funaki, T. Hashimoto, K. Makita, Y. Tanaka and Y. Ikeda, "Compact Helicon Source Experiments for Electrodeless Electromagnetic Thruster", AIAA-2007-5311, 43rd Joint Propulsion Conference & Exhibit, Jul., Cincinnati, OH, USA, 2007.

¹⁵K. Toki, T. Seto and N. Asakura, "Primitive Experiments on Photon Pressure Space Propulsion - Energy Direct Conversion to Thrust ", AIAA-2007-5260, 43rd Joint Propulsion Conference & Exhibit, Jul., Cincinnati, OH, USA, 2007.

¹⁶Y. Takao and K. Ono: "Miniature electrothermal thruster using microwave-excited plasmas: A numerical design consideration", *Plasma Sources Sci. Technol.* **15**(2), 211-227 (2006).

¹⁷Y. Takao, K. Ono, K. Takahashi, and Y. Setsuhara: "Microwave-sustained miniature plasmas for an ultra small thruster", *Thin Solid Films* **506-507**, 592-596 (2006).

¹⁸Y. Takao, K. Ono, K. Takahashi, and K. Eriguchi: "Plasma Diagnostics and Thrust Performance Analysis of a Microwave-Excited Microplasma Thruster", *Jpn. J. Appl. Phys.* **45**(10B), 8235-8240 (2006).

¹⁹Y. Takao, K. Eriguchi, and K. Ono: "A miniature electrothermal thruster using microwave-excited microplasmas: Thrust measurement and its comparison with numerical analysis", *J. Appl. Phys.* **102** (2007) (in press).

²⁰Nishida, S., Kawamoto, S., Okawa, Y., Terui, F., and Kitamura, S., "Space Debris Removal System using a Small Satellite," 57th International Astronautical Congress, IAC Paper 06-B6.4.02, Valencia, Spain, October 2006.

²¹Ikeda, T., Yamagiwa, Y., Kawamoto, S., Ohkawa, Y., Nishida, S., and Nakajima, A., "Development of Electrodynamic Tether Using Simple Reel Mechanism", Proceedings of 25th International Symposium on Space Technology and Science, Kanazawa, ISTS-2006-s-03, 2006, pp. 1-6.

²²Nakamura, Y., Yamagiwa, Y., Ohkawa, Y., Kawamoto, S., Nishida, S., and Kitamura, S., "Environmental Effects on Electron Emission Characteristics of Carbon Nanotube Cathodes", Proceedings of 25th International Symposium on

Space Technology and Science, Kanazawa, ISTS-2006-s-18, 2006, pp. 1-6.

²³Ikeda, T., Nakamura, Y., Yamagiwa, Y., Kawamoto, S., Ohkawa, Y., Nakajima, A., "Multiple Bare Tethers for Electrodynamic Tether Propulsion", IEPC2007. (will be presented)

²⁴Yamagiwa, Y., Fukui, K., and Otsu, H., "Evaluation of the Performance of LEO-GEO Hybrid Tether Orbit Transfer System", Aerospace Science and Technology. (submitted)

²⁵Yamagiwa, Y., Watanabe, S., Kotanagi, K., and Otsu, H., "Innovative Interplanetary Transportation System Using Electrodynamic tether and Magnetic Coil," Proceedings of 25th International Symposium on Space Technology and Science, Kanazawa, ISTS-2006-b-46, 2006, pp. 1-5.

²⁶Nakanishi, T., Yamagiwa, Y., Otsu, H., Nishimura, T., and Mizuno, A., "Experimental Study on Space Propulsion Using Solid Micro-Particles as Propellant", Space Transportation Symposium 2007, Sagamihara, 2007. (in Japanese)

²⁷Aoyagi, J., Takegahara, H., Kuriki, K., *et al.*, "A Preliminary Study On Hydrazine Decomposition By Discharge Plasma," International Astronautical Congress, Fukuoka, Japan, IAC-05-C4.P.07, October 17-21, 2005.

²⁸Aoyagi, J., Takegahara, H., Kuriki, K., *et al.*, "Evaluation on Hydrogen Peroxide Decomposition with Discharge Plasma," International Symposium on Space Technology and Science (ISTS), 2006-a-36, Kanazawa, Japan, May 30- June 6, 2006.

²⁹Katayama, T., Hatakeyama, T., Takegahara, H., *et al.*, "Effects of Environmental Conditions to Discharge Characteristics of Hollow Cathode," ISTS, 2006-b-24 Kanazawa, Japan, May 30- June 6, 2006.

³⁰A. Sasoh, Department of Aerospace Engineering Nagoya University, Nagoya, Japan; K. Anju, K. Suzuki, M. Shimono and K. Sawada, "Time- resolved and Integrated Laser Ablative Impulse Performance of Polyacetal," AIAA paper, AIAA-2007-4389.

³¹Horisawa H., Noda, T., Onodera, K., and Kimura, I., "Microfabrication of Quartz Micro-Arcjet Nozzles with a Fifth-HG Nd:YAG Laser," AIAA Paper 2005-4075, 2005.

³²Horisawa H., Noda, T., Onodera, K., and Kimura, I., "Micro-Arcjet: Microfabrication with UV Lasers and Thrust Characteristics," 29th International Electric Propulsion Conference Paper, IEPC-2005-123, 2005.

³³Horisawa, H., Onodera, K., Noda, T., and Kimura, I., "Multi-Jet Effects of Micro-Nozzle Array in Very Low-Power DC Micro-Arcjets," AIAA Paper 2006-4496, 2006.

³⁴S. Yokota, K. Komurasaki, Y. Arakawa, "Plasma Density Fluctuation inside a Hollow Anode in an Anode-layer Hall Thruster," 42nd Joint Propulsion Conference, Sacramento, 2006, AIAA-2006-5170.

³⁵N. Nagao, S. Yokota, K. Komurasaki, Y. Arakawa, "Development of a Dual Pendulum Thrust Stand for Hall Thrusters," 43rd Joint Propulsion Conference, Cincinnati, 2007, AIAA-2007-5298.

³⁶M. Matsui, S. Yokota, D. Sakoh, K. Komurasaki and Y. Arakawa, "Number Density Distributions of Xenon Atom in Hall Thruster Plumes," 43rd Joint Propulsion Conference, Cincinnati, 2007, AIAA-2007-5306.

³⁷Kakami, A., Koizumi, K., Komurasaki, K., and Arakawa, Y., "Design and Performance of Liquid Propellant Pulsed

Plasma Thruster," *Vacuum*, Vol.73 (2004) No.3-4, pp.419-425.

³⁸Koizumi, K., Komurasaki, K., and Arakawa, Y., "Development of Thrust Stand for Low Impulse Measurement from Microthrusters," *Review of Scientific Instruments*, Vol.75 (2004) No.10, pp.3185-3189.

³⁹Koizumi, H., Noji, R., Komurasaki, K., and Arakawa, Y., "Plasma acceleration processes in an ablative pulsed plasma thruster," *Physics of Plasmas*, Vol.14 (2007) No.3, Article No. 033506.